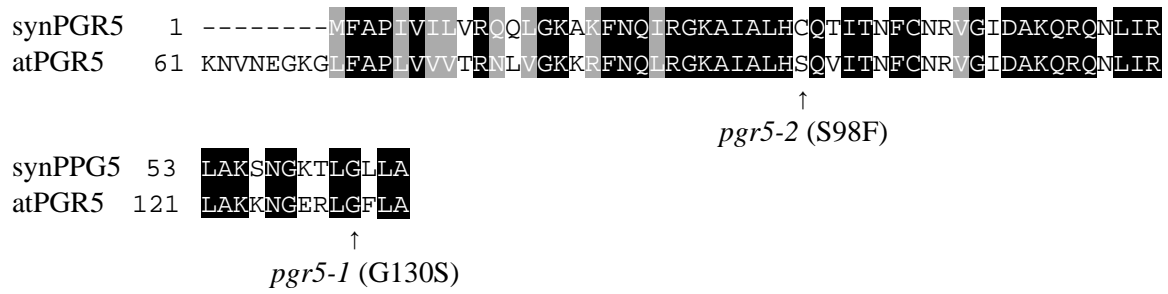


# **Supplementary Information**

**Evidence that cyanobacterial Sll1217 functions analogously to PGRL1 in enhancing PGR5-dependent cyclic electron flow**

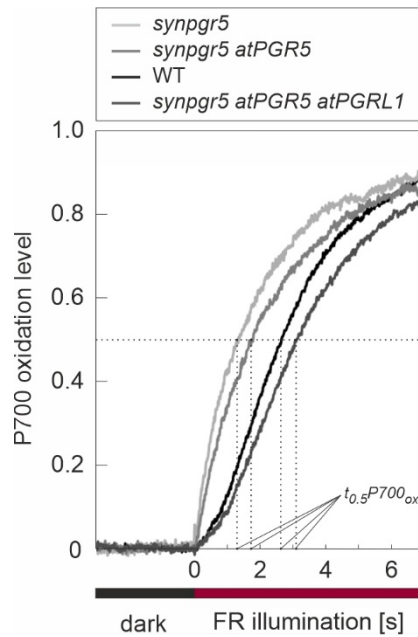
Dann & Leister

Nature Communications, 2019



**Supplementary Figure 1** PGR5 protein alignment and positions of mutation in atPGR5.

The sequence of the mature atPGR5 protein<sup>1</sup> was aligned with synPGR5 (Ssr2016) using MUSCLE<sup>2</sup>. Identical/similar amino acids are highlighted by black/grey shading. The positions of published non-synonymous mutations in atPGR5 are annotated relative to start codon in the precursor protein with cTP. The homology between the two proteins is 45%/56% identity/similarity at the amino acid level; it increases to 65%/80% when only the region from aa 69 to aa 133 of atPGR5 is considered.



**Supplementary Figure 2** Determination of  $t_{0.5P700_{ox}}$  for representative *Synechocystis* strains. Dark-incubated cultures (normalized to equal  $OD_{730\text{ nm}}$  values) were subjected to 3 s of dark/measuring light illumination to determine P700<sup>+</sup> baseline absorbance, followed by 60 s of FR illumination to induce P700 oxidation and reach steady-state oxidation levels. Baseline absorbance was set to 0, while absorbance maxima were set to 1, respectively. For each measurement, the rate constant for maximum P700 oxidation was determined as the time point ( $t_{0.5P700_{ox}}$ ) at which the baseline corrected/normalized oxidation curves exceeded 0.5 for the first time. Mean values of  $t_{0.5P700_{ox}}$  and standard deviations thereof were determined for all genotypes and employed as a proxy for CEF activity (see text).

**a**

>s110622 quinolinate synthetase  
Length = 318

Score = 28.1 bits (61), Expect = 0.65, Method: Compositional matrix adjust.  
Identities = 12/38 (31%), Positives = 20/38 (52%)

Query: 123 KEELMWEGSSVVMLSSDEQRFLEASMAVYVSGNPILNDE 160  
+E ++W+GS +V + E+R LE Y I + E  
Sbjct: 173 REMVLWQGSCIVHETFSERRLLELKTQYPQAEIIAHPE 210

**b**

>s111217 unknown protein  
Length = 225

Score = 25.8 bits (55), Expect = 1.1, Method: Compositional matrix adjust.  
Identities = 13/41 (31%), Positives = 23/41 (56%), Gaps = 1/41 (2%)

Query: 16 SNVLPYCSI-NKAEKKTIGEMEQEFLQALQSFYDYGKAIMS 55  
+N +PY NKA + E + F++ L F++ GK I++  
Sbjct: 103 TNTVPYKPPENKAYSVKVKERFRPFVEQLLVFHWQGKQIIT 143

**c**

```

synNADA      1  -----MFTAVAPPQETLPRDLVGATQSLKKELNAVILAHYYQEAAIQDIADY-
atPGRL1A    61  ATTEQSGPVGGDNVDSNVLPYCSINKAEKKTIGEMEQEFLQALQSFYDYGKAIMSNEEFD
atPGRL1B    50  ASTDQSGQVGGEEVDSKILPYCSINKNEKRTIGEMEQEFLQALQSFYEGKAIMSNEEFD

synNADA     48  -LGDSL---GLSQQAASTADADVIVFAGVHFMAETAKLLNP--HKLVLPLDLEAGCSLADS
atPGRL1A   122  NLKEELMWEGSSVVMLSSDEQRFLEASMAVYVSGNPILNDEEYDKLKLKLDGSDIVSEG
atPGRL1B   111  NLKEELMWEGSSVVMLSSDEQRFLEASMAVYVSGNPILSDEEYDKLKLKMDGSEIVCEG

synNADA    102  --CPPREFAEFKQRHPDHLVLSYINCTAETKALSDIIC---TSNAVKIVQQLPPDQKII
atPGRL1A   182  PRCSLRSKKVYSDLAVDYFKMLLNVPATVVALGLFFFLDDIIGFETYSMELPEPYSFI
atPGRL1B   171  PRCSLRSKKVYSDLAIDYFKMFLNVPATVVALGLFFFLDDIIGFETYSLELPEPFSFI

synNADA    157  FAPDRNLGRYVMEQTGREMVLWQGS--CIVHETFSERLLELKTQYPQAEIIAHPECEKA
atPGRL1A   242  FT-----WFAAVPVIVYLALSITKLI-----IKDFLILKGP-CPNC
atPGRL1B   231  FT-----WFAAVPAIVYLALSITKLI-----LKDFLILKGP-CPNC

synNADA    215  ILRHADFIGSTTALLNYSQKQKEFIVGTEPGIIHQMEKLSPSKQFIPPPNNSNCD---
atPGRL1A   277  GTENTSFFGT-----ISSSSGKKTNTVK
atPGRL1B   266  GTENVSEFGT-----ISSPNSNTNNVK

synNADA    272  CNECPYMLRLNTLEKIYWAMQRRSPEITLPEATMAAALKPIQRMLAMS
atPGRL1A   301  CTNC-----GTAMVY---DSGSRLITLPECSQA-----
atPGRL1B   290  CSGC-----GTEMVY---DSGSRLITLPECGKA-----

```

**d**

```

Sll1217      1  -MSELQTLIRTIHQEAEREPP-PIIDSPIYEQACK-----DAIDPILFEGG-----
atPGRL1A    61  ATTEQSGPVGGDNVDSNVLPPYCSINKAEEKKTIQEMEQEFLQALQSFYMDGKAIMSNEEFD
atPGRL1B    50  ASTDQSGQVGGEEVDISKILPPYCSINKNEKRTIQEMEQEFLQAMQSFYMEGKAIMSNEEFD

Sll1217     43  NLGSQLCFFGRD---LGADDEVROGQPLIG--AAGRLLVRKGFFFAWQGRVPRGQDDIQTVC
atPGRL1A    121  NLKEELMWEQSSVVMVLSSEDEQRFLEASMAAYVSNPILNDEEYDKLKLKIKIDGSDIVSEG
atPGRL1B    110  NLKEELMWEQSSVVMVLSSEDEQRFLEASMAAYVSNPILSDEEYDKLKMKIKMDGSETVCEG

Sll1217     98  QRILLTNTVPYKPPENKAYSVKVKERFRPFVEQLLVFHWQ---CKQIITLTGT--EATK--
atPGRL1A    181  PRCSLRSKKVYSDLAVDYFKMLLLNVPATVVALGLFFFLDDITGFEITYIMELPEPYSFI
atPGRL1B    170  PRCSLRSKKVYSDLAIDYFKMFLNVPATVVALGLFFFLDDITGFEITYILELPEPYSFI

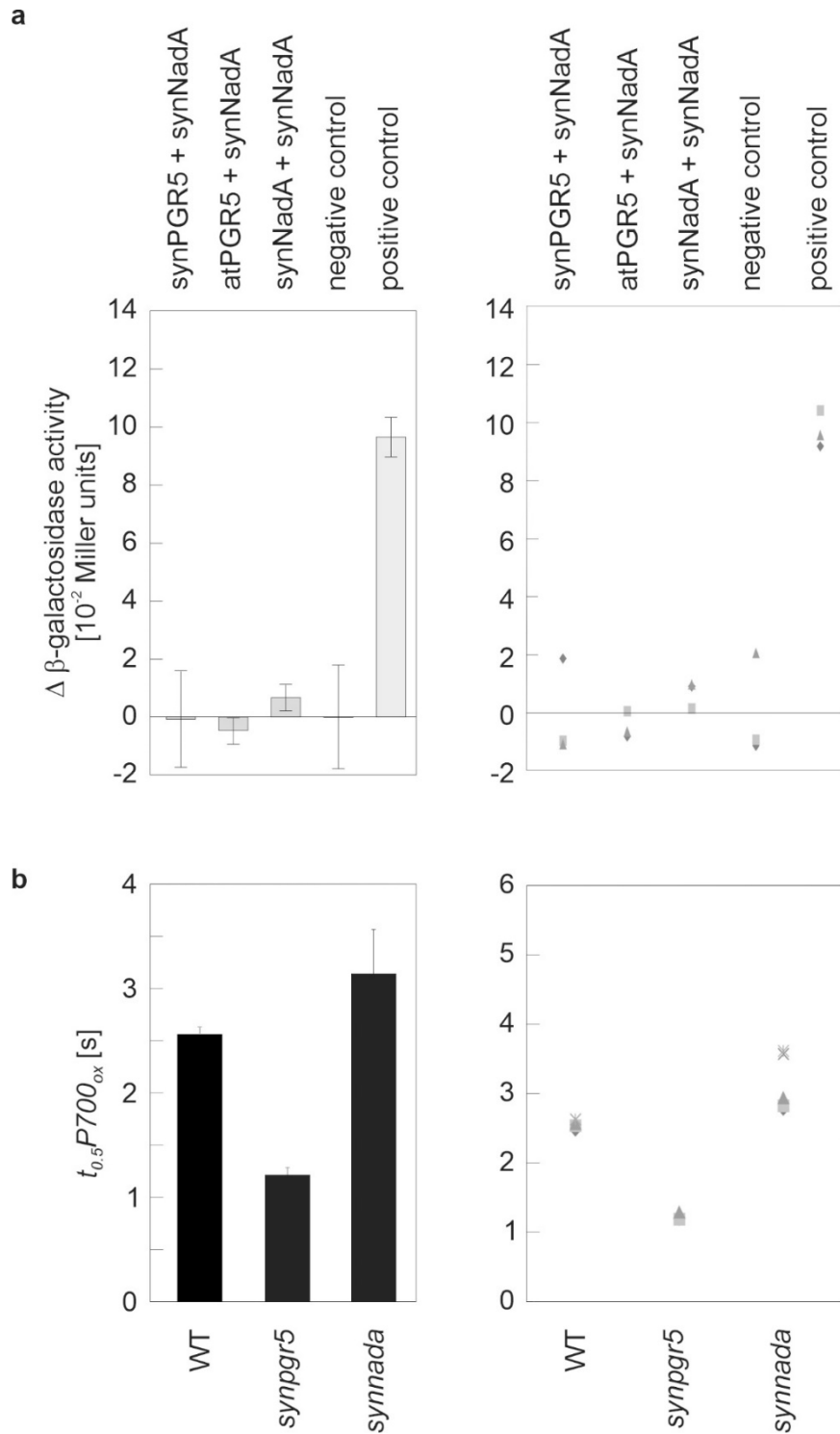
Sll1217    151  --WFAP-----YAPKGQLDEFFQGGDRYECSLDVLIKAKTAAGKGSQKIV---RLMPLPH
atPGRL1A    241  FTWFAAVPVIVYLLALSITKLIK-----DFLLKGPVPCNCGENTSFSGTILSSSS
atPGRL1B    230  FTWFAAVPAIVYLLALSITKLIK-----DFLLKGPVPCNCGENVSFFGTILSSIPN

Sll1217    201  PSPLNKRYYGQFPIML-----QRRLTEIAF----
atPGRL1A    292  GGKTNIVKCTNCGTAMVYDSGSRLITLPEGSQA
atPGRL1B    281  DSNTINNVKCSGCGTEMVYDSGSRLITLPEGGKA

```

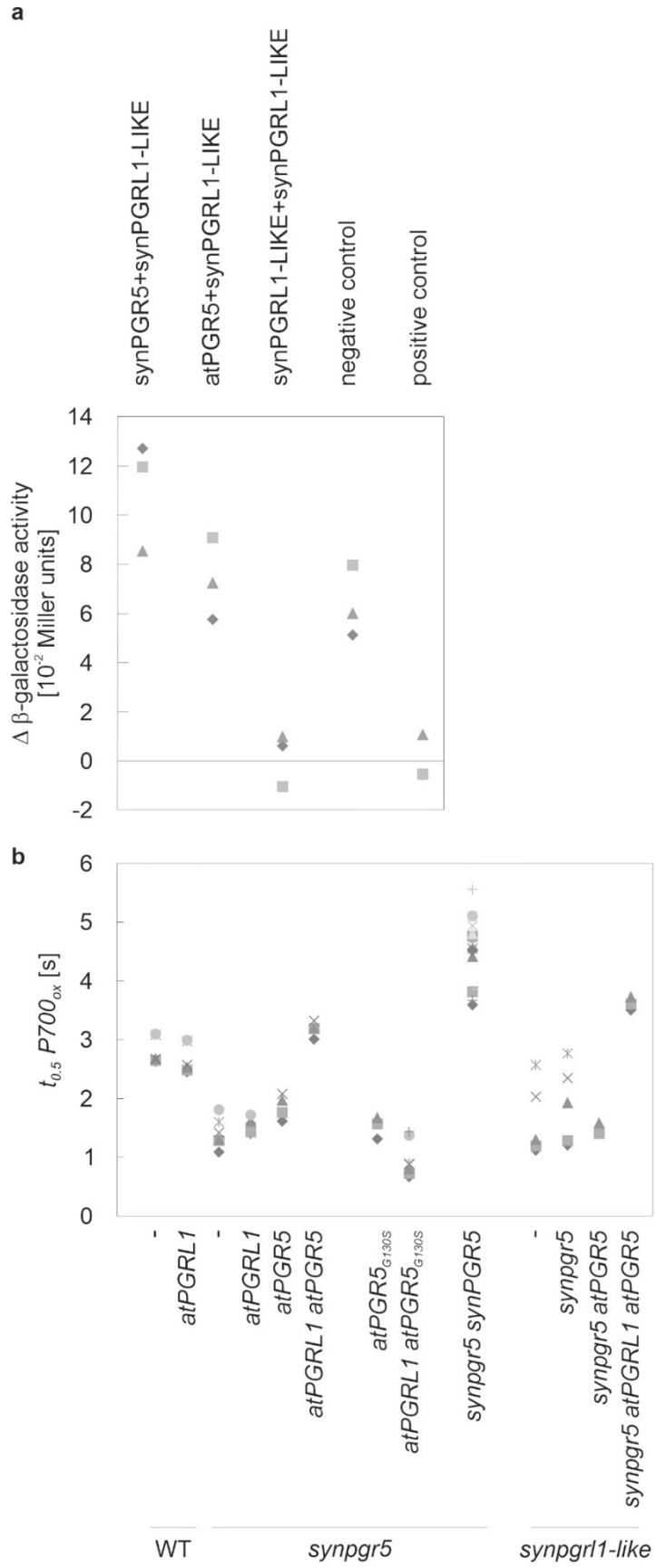
**Supplementary Figure 3** Short stretches of Sll0622/synNadA and Sll1217/synPGRL1-LIKE share limited sequence similarity with PGRL1.

**a, b** Original CyanoBase<sup>3</sup> pblast hits for synNadA and Sll1217/synPGRL1-LIKE were obtained using either the complete sequence of the mature atPGRL1A protein or its N-terminal region (between cTP and first TM region) only. **c, d** Alignments of full-length Sll0622 and Sll1217 and mature PGRL1 proteins from *Arabidopsis thaliana* (without cTPs) generated using MUSCLE<sup>2</sup>. The Sll0622 protein shares 13.8%/ 26.8% and 15.0%/27.7% identity/similarity at the amino-acid level with atPGRL1A and atPGRL1B, respectively. The Sll1217 protein shares 13%/29% and 14%/28% identity/similarity at the amino-acid level with atPGRL1A and atPGRL1B, respectively. Conserved cysteine residues in PGRL1 proteins<sup>4</sup> are highlighted in green, the three cysteine residues present in Sll1217 are highlighted in cyan.

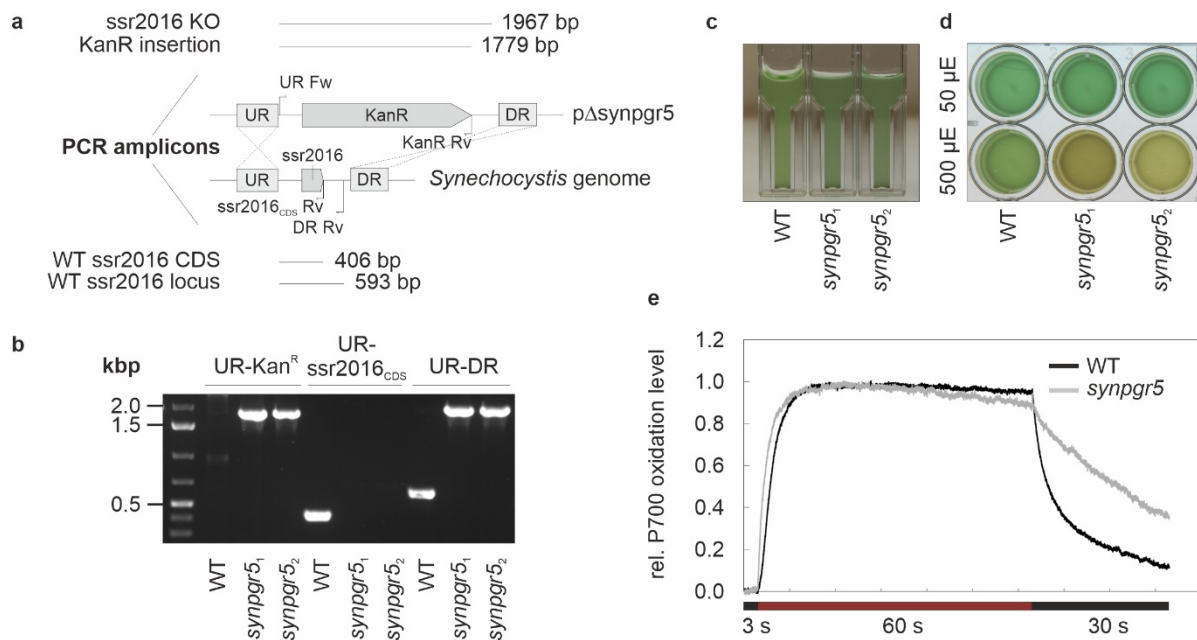


**Supplementary Figure 4** The synNadA protein is not a functional PGRL1 analogue.

**a** The synPGR5 and synNadA proteins do not physically interact. Bacterial two-hybrid analyses were performed as described in Fig. 3a. **b** Lack of synNadA does not affect CEF, as determined by P700 oxidation measurements. Data are provided as averages with standard deviations (left) and dot plots (right). Sample sizes  $n$  were 3 for B2H assays (**a**) and 5/3/5 for  $t_{0.5}P700_{ox}$  of WT, *synpgr5* and *synnada* (**b**).



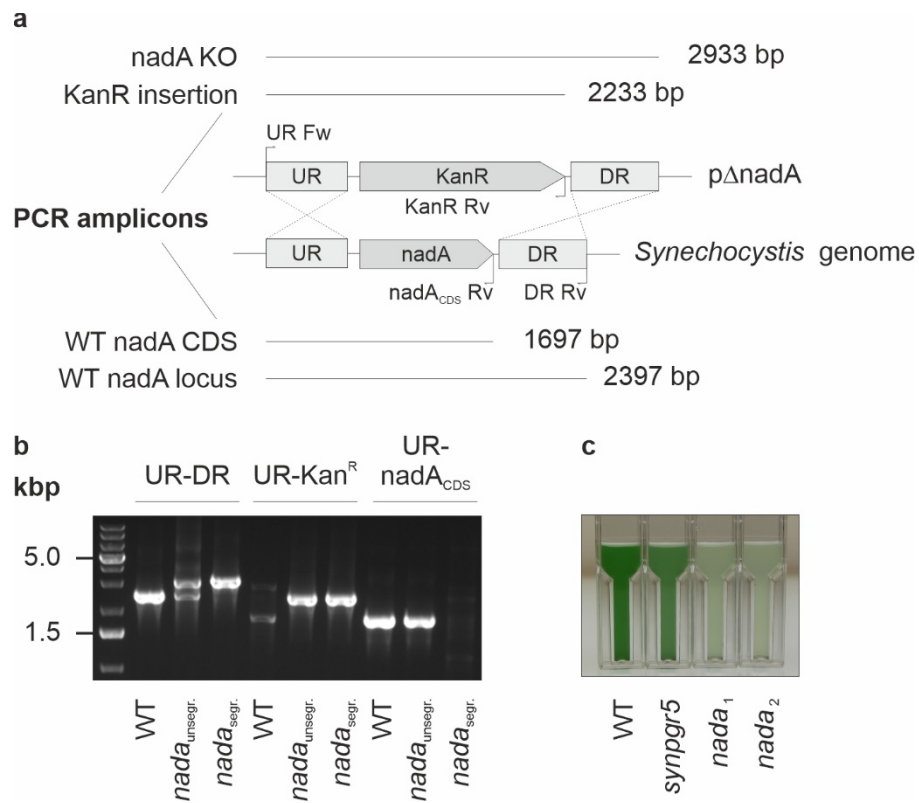
**Supplementary Figure 5** Dot plots for the data shown in Fig. 3a (a) and Fig. 3c (b).



**Supplementary Figure 6** Generation of an *ssr2016* knockout mutant (*synpgr5*).

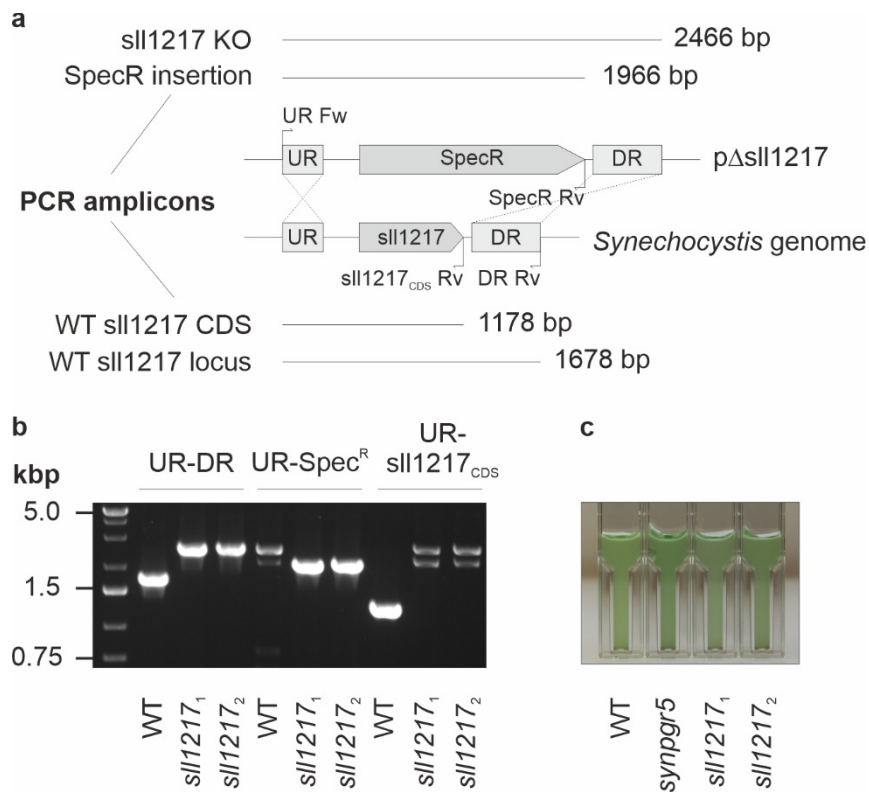
**a,b** Genomic replacement of the *ssr2016* ORF by a KanR cassette and full segregation were confirmed by PCR. Genotyping primer binding sites and 5'-3' orientation are indicated by labeled arrows; expected amplicon origins and sizes are indicated. Under low (**c**; 30 μE) to ambient light (**d**; 50 μE) no obvious deviation from WT cells was observed. However, enhanced susceptibility to high light intensities (**d**; 500 μE) and accelerated P700 oxidation/delayed P700 re-reduction upon on-/offset of FR light was observed (**e**), confirming the findings of former studies conferred with a gene interruption mutant of *ssr2016* (SM2016)<sup>5</sup>. P700 oxidation curves (**e**) represent averages over all measurements of the respective genotypes represented in Fig. 1c.





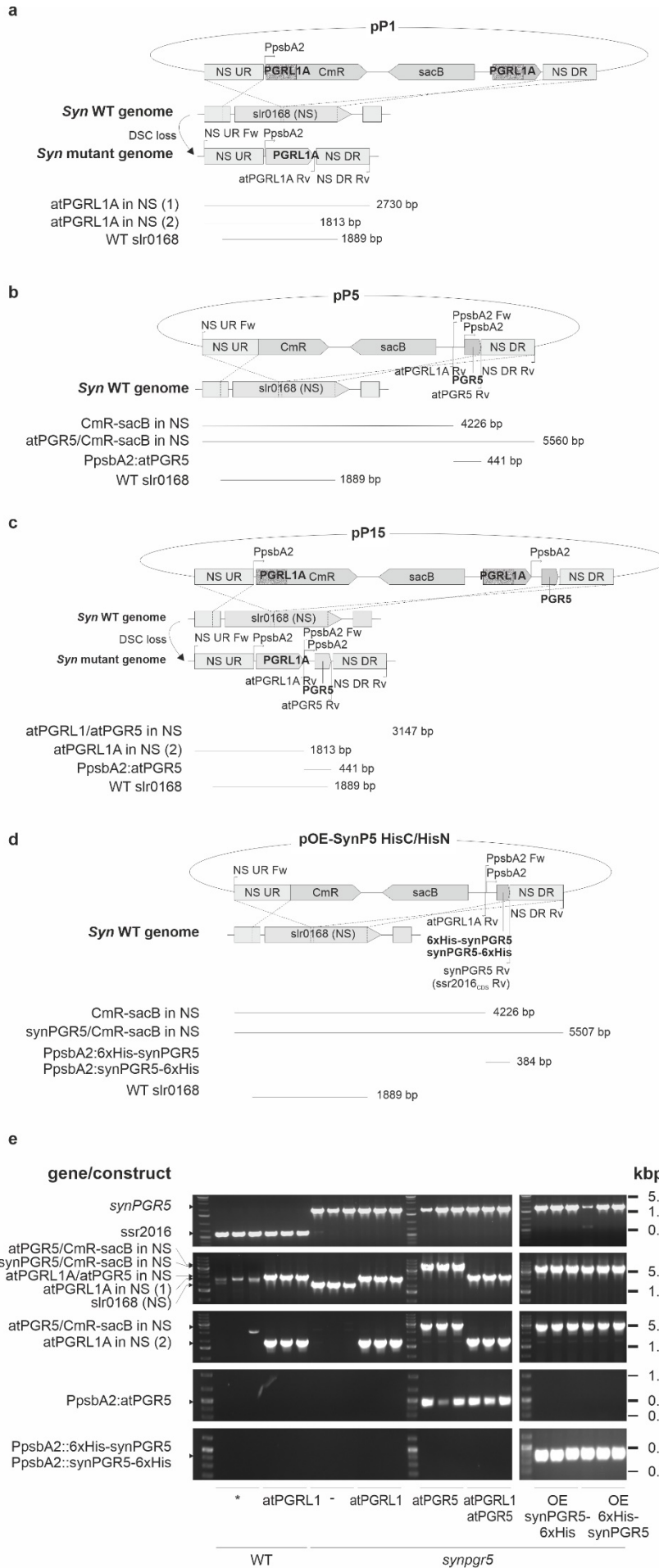
**Supplementary Figure 7** Generation and initial phenotypical assessment of a *nada* knockout mutant.

**a** The genomic ORF encoding NadA (sll0622) was replaced with a KanR cassette by homologous recombination. **b** Segregation of the *nada* mutation was confirmed by PCR. Genotyping primer binding sites and 5'-3' orientation are indicated by labeled arrows; expected amplicon origins and sizes are indicated. **c** Under low light (30  $\mu$ E) obvious deviation from WT and *synpgr5* cells was observed in terms of pronounced paleness of *nada* cultures.



**Supplementary Figure 8** Generation and initial phenotypical assessment of an *sll1217*-knockout mutant.

**a** The genomic ORF *sll1217* was replaced with a SpecR cassette by homologous recombination. **b** Segregation of the *sll1217* mutation was confirmed by PCR. Genotyping primer binding sites and 5'-3' orientation are indicated by labeled arrows; expected amplicon origins and sizes are indicated. **c** Under low light (30  $\mu$ E) no obvious deviation from WT and *synpgr5* cells was observed.



**Supplementary Figure 9** Generation of atPGR gene expression strains in *Synechocystis*.

**a-d** Expression constructs were introduced into a genomic neutral site, ORF slr0168, by homologous recombination using a non-replicative vector as shuttle. When appropriate, chloramphenicol resistance (CmR) – sacB double selection cassettes were removed by negative selection on 5 % (w/v) sucrose agar as described earlier<sup>6</sup>. Redundant PGRL1A gene sequences for intrachromosomal recombination are displayed in grained grey. Genotyping primer binding sites and 5'-3' orientation are indicated by labeled arrows; expected amplicon origins and sizes are indicated. **e** Genotyping PCR of three independent transformants each confirmed *synpgr5* genetic background, as well as transgene cassette presence and segregation status. Note that the WT control does not display an slr0168 amplicon of the expected size (2183 bp) because of complete deletion of the slr0168 CDS by replacement with a KanR selection cassette.

**Supplementary Table 1** Primers used in this study.

Primer	genotyping short name	Supplementary Figure (Sup Fig.)	Sequence (5'-3')
backbone_fwd			ACCTGGGCCCCTGCATCC
backbone_rev			GCTTACCTGTTTAAACTATCAGTG
ssr2016_UR_fwd	UR Fw	Sup Fig. 6	<b>gatagtttaaacaggttaagc</b> CCGGGTAATCCGGGTGGC
ssr2016_UR_rev			<b>ggcggaacatggcagtgact</b> CCTAAATTCCTACG
KanR_Cass_fwd	KanR Rv		caacgctcgggtgccgccggcggttttTTTGGTCTCACGTTGGAATTC
KanR_Cass_rev			aaacgaagagGTAAACAGCCAGCGCTG
ssr2016_DR_fwd			gctgttttacCTCTTCGTTTTCAATAATTCTTGCCAAAC
ssr2016_DR_rev	DR Rv		tgatgacagtgggcccaggtTTCCACCGAAGGGCTGG
<i>B2H ssr2016 Rv</i>	<i>ssr2016_CDS Rv</i>		<i>tcagattctagaTTAGGCCAATAAACCGAG</i>
nadA_UR_fwd	UR Fw		Sup. Fig. 7
nadA_UR_rev		acgtgagacaaaTATGTTTTCGGCTCCTGGAATATTTATAG	
KanR_fwd		gagccgaacataTTTGGTCTCACGTTGGAATTC	
KanR_rev	KanR Rv	gattatgccaccGTAAACAGCCAGCGCTG	
nadA_DR_fwd		ctggctgtttacGGGTGGCATAATCAGGCTC	
nadA_DR_rev	DR Rv	tggggtggatgcagtgggcccaggtTATTGCCACTAGAATTAGCCG	
<i>B2H sll0622 Rv</i>	<i>nadA_CDS Rv</i>	<i>accaccgaattcCTAGGACATGGCCAGC</i>	
sll1217_UR_fwd	UR Fw	Sup. Fig. 8	
sll1217_UR_rev			tgttctctagagGGAAGAACTGAGATAACTGATTG
SpecR_fwd			agtttctccCTCTAGAAGAACAGCAAGGCCG
SpecR_rev	SpecR Rv		aagtctggaaGCCGCTCAATTCGCTGCG
sll1217_DR_fwd			attgagcggcTTCCAGACTTAAAATATTTATCACCTTACTTC
sll1217_DR_rev	DR Rv		tgatgacagtgggcccaggtCCGCACAATGGTGTAGGG
<i>B2H sll1217 Rv</i>	<i>sll1217_CDS Rv</i>		<i>gtagtcggtaccCTAGAAAGCAATTTCCGTTAAGCG</i>

Uppercase letter indicate specifically annealing sites; lowercase letters indicate complementary overhangs; red indicates not complementary sites and linear assembly was blunt-ligated; italics indicates B2H primer used for genotyping. The vector backbone was pICH69822

## Supplementary References

1. Sugimoto, K., *et al.* A single amino acid alteration in PGR5 confers resistance to antimycin A in cyclic electron transport around PSI. *Plant Cell Physiol* **54**, 1525-1534 (2013).
2. Edgar, R. C. MUSCLE: multiple sequence alignment with high accuracy and high throughput. *Nucleic Acids Res* **32**, 1792-1797 (2004).
3. CyanoBase, <http://genome.microbedb.jp/cyanobase>.
4. Hertle, A. P., *et al.* PGRL1 is the elusive ferredoxin-plastoquinone reductase in photosynthetic cyclic electron flow. *Mol Cell* **49**, 511-523 (2013).
5. Yeremenko, N., *et al.* Open reading frame *ssr2016* is required for antimycin A-sensitive photosystem I-driven cyclic electron flow in the cyanobacterium *Synechocystis* sp. PCC 6803. *Plant Cell Physiol* **46**, 1433-1436 (2005).
6. Viola, S., Rühle T. & Leister D. A single vector-based strategy for marker-less gene replacement in *Synechocystis* sp. PCC 6803. *Microb Cell Fact* **13**, 4 (2014).